

SODIUM NITRATE FOR HIGH TEMPERATURE LATENT HEAT STORAGE

T. Bauer, D. Laing, U. Kröner, R. Tamme

Institute of Technical Thermodynamics, German Aerospace Center (DLR)
Pfaffenwaldring 38-40, 70569 Stuttgart, Germany
Tel. +49-711-6862-681, thomas.bauer@dlr.de

ABSTRACT

In this paper the results of material investigations of sodium nitrate (NaNO_3) with a melting temperature of $306\text{ }^\circ\text{C}$ as a phase change material (PCM) are presented. The thermal stability was examined by long duration oven tests. In these experiments the nitrite formation was monitored. Although some nitrite formation in the melt was detected, results show that the thermal stability of NaNO_3 is sufficient for PCM applications. The compatibility of graphite foil and molten NaNO_3 was also examined. Results show that the molten NaNO_3 oxidizes graphite. Measurements on thermophysical properties of NaNO_3 are also reported. These properties include the thermal diffusivity by the laser flash method and the heat capacity by a heat flux differential scanning calorimeter. Reliable temperature dependent thermophysical values of the density, heat capacity, diffusivity and conductivity are identified. Results show that there is a lack of consistent conductivity and diffusivity data in the solid phase.

1. INTRODUCTION

This paper considers the latent heat storage concept using phase change materials (PCMs). PCMs are in particular advantageous for two phase heat transfer fluids. In this concept, both the heat carrier and the PCM undergo a phase change at approximately the same temperature.

Our ongoing research focuses on high temperature latent heat storage designs for the two phase heat carrier water-steam in the temperature range 120 to $350\text{ }^\circ\text{C}$. The condensation and evaporation temperature of the carrier is pressure dependent and occurs between $120\text{ }^\circ\text{C}$ (2 bar) and $350\text{ }^\circ\text{C}$ (165 bar). Depending on the water-steam pressure, a suitable PCM needs to be identified [1]. Appropriate PCMs for this temperature range are anhydrous alkali nitrate/nitrites and their mixtures, if requirements such as handling, thermal stability, steel compatibility and economic aspects are taken into account [2]. The research focuses on latent heat storage systems for industrial process heat utilization in the low temperature range (120 - $250\text{ }^\circ\text{C}$) and solar thermal power generation in the high temperature range (250 - $350\text{ }^\circ\text{C}$). Solar thermal power technologies using optical systems for concentration of sunlight can be classified into dish, tower and through systems. An example where sodium nitrate (NaNO_3) could be utilized as PCM are direct steam generating parabolic troughs. These systems aim for a pressure of around 100 bar. At this pressure the water-steam phase change occurs at a temperature of around $310\text{ }^\circ\text{C}$. This temperature suits the melting temperature of NaNO_3 .

2. GENERAL ASPECTS AND PHASE TRANSITIONS OF SODIUM NITRATE

Sodium nitrate (NaNO_3) is found in naturally occurring deposits. These deposits contain various other salts and require processing to obtain pure NaNO_3 . On a large scale, NaNO_3 -rich deposits in Chile are exploited. Smaller but also significant quantities are produced synthetically [3,4].

The colorless or white crystalline salt has a molar mass of $84,99\text{ g/mol}$. NaNO_3 is very soluble in water. It is hygroscopic, but does not form hydrated solid phases. The two major grades of

NaNO₃ are technical and agricultural. NaNO₃ is used as a fertilizer as well as in a number of industrial processes. The industries include glass, enamel, porcelain, explosives and charcoal briquettes manufacturing. Some grades of NaNO₃ contain anticaking agent. Molten salt mixtures containing NaNO₃ are employed as heat-treatment baths, as heat transfer fluids and as sensible heat storage media [3,4].

Lumdsen and Jirri reviewed experimental data of the **melting temperature** and the **melting enthalpy** of pure NaNO₃ [5,6]. Both authors report the average melting temperature at 306 °C. The reported enthalpy data vary stronger in a range from 172 to 187 J/g [5,6]. The average values are 177 J/g [5] and 178 J/g [6]. NaNO₃ has been also considered for differential scanning calorimeter (DSC) calibration with a recommended value of 178 J/g [7]. There is some larger discrepancy in terms of **the second order transition enthalpy** at around 275 °C. Values from 12 J/g (drop calorimeter) to 45 J/g (DSC) are reported [6]. An experimental difficulty with molten NaNO₃ is the **creeping** tendency. Here, a thin film of molten salt forms on the surface. The salt wets and spreads spontaneously on many crucible surfaces [8, 9].

3. THERMAL STABILITY OF SODIUM NITRATE AND NITRITE FORMATION

The thermal decomposition of NaNO₃ can be divided in three characteristic regions [10-16]:

1. Little nitrite formation: Above the melting temperature (T_m) to about 450 °C
2. Nitrate-Nitrite equilibrium: about 450 °C to 700 °C
3. Decomposition of the nitrite with release of nitrogen oxides above 700 °C

Literature about the **low temperature** region (T_m to 450 °C) is generally limited. Kust reported about experiments of the eutectic KNO₃-NaNO₃ with $T_m = 222$ °C. They found small amounts of nitrites at temperatures as low as 295 °C in the melt. Due to the experimental procedure it was assured that this nitrite was not due to impurities in the nitrate. The nitrite ion concentration reached equilibrium within 7 to 16 hours at temperatures between 295 and 340 °C [13].

To improve the data basis for the thermal stability of NaNO₃ in the low temperature region, long-duration test of NaNO₃ at 350 °C were performed at the DLR. The NaNO₃ was purchased from BASF. The technical non-food grade salt has a purity of min. 99 %. The major impurities are NaNO₂ (50), Na₂CO₃ (400), NaCl (250) and Na₂SO₄ (300) with maximum values in mg/kg. The salt was heated in a borosilicate glass beaker which was placed in a batch furnace (air at atmospheric pressure). For nitrite analysis, the melt was dissolved in deionised water. Mass losses of the melt were monitored with an analytical balance at room temperature. The results show that about 0.1 wt% NO₂⁻ forms within a few hours in the melt. This value remains constant within 24 hours. The value increases to 0.2 to 0.25 wt% NO₂⁻ after about 2600 hours. The first melting cycle showed mass losses from 0.1 to 0.3 wt%. This loss is attributed to moisture in the salt. Mass variations during the 2600 hour were monitored four times and were found to be smaller than +/-0.05 wt%. Overall, the measurements showed that NaNO₃ is thermally stable at 350 °C and that small amounts of nitrite are formed.

It is well known that molten nitrates decompose to nitrites in the **intermediate temperature region** from about 450 to 700 °C. The thermal dissociation is reversible and the equilibrium reaction can be written for NaNO₃ as follows [8,11-16].



Kinetic data of the oxidation and the decomposition of different alkali metal nitrates have been reported. They include $\text{KNO}_3/\text{KNO}_2$ [10-12,15], $\text{KNO}_3\text{-NaNO}_3/\text{KNO}_2\text{-NaNO}_2$ [8,12] and $\text{NaNO}_3/\text{NaNO}_2$ [12,15]. The time to reach equilibrium depends on parameters such as the reaction direction (decomposition or oxidation), the atmosphere and the experimental setup (usually bubbling of gas through the melt). At higher temperatures the equilibrium is reached generally faster compared to lower temperatures. The reported times range from days at low temperatures to tens of minutes at high temperatures.

In the following, we describe examinations of the effect of **nitrite impurities on the melting behaviour** of NaNO_3 . A known method for purity determination is the use of the van't Hoff law. This law describes the melting temperature reduction due to impurities, where $R = 8.31441 \text{ J}/(\text{mol}\cdot\text{K})$ is the molar gas constant, H_2 the melting enthalpy (J/mol) and T_2 the melting temperature (K) of the pure material, T the temperature where the impure material is completely liquid (K) and $x_{1(T)}$ the molar fraction of the impurity (Figure 1, right). Figure 1 on the left shows two DSC-measurements carried out by the DLR. Compared to pure NaNO_3 , it can be seen that due to the addition of NaNO_2 the melting range broadens and the melting temperature is reduced. Bader presents a method to calculate the DSC heat flux depending on the impurity fraction [17]. Figure 1 on the right shows the calculation for NaNO_3 . DSC-measurement and this calculation show a good agreement considering that no desmearing of the DSC-signal was applied.

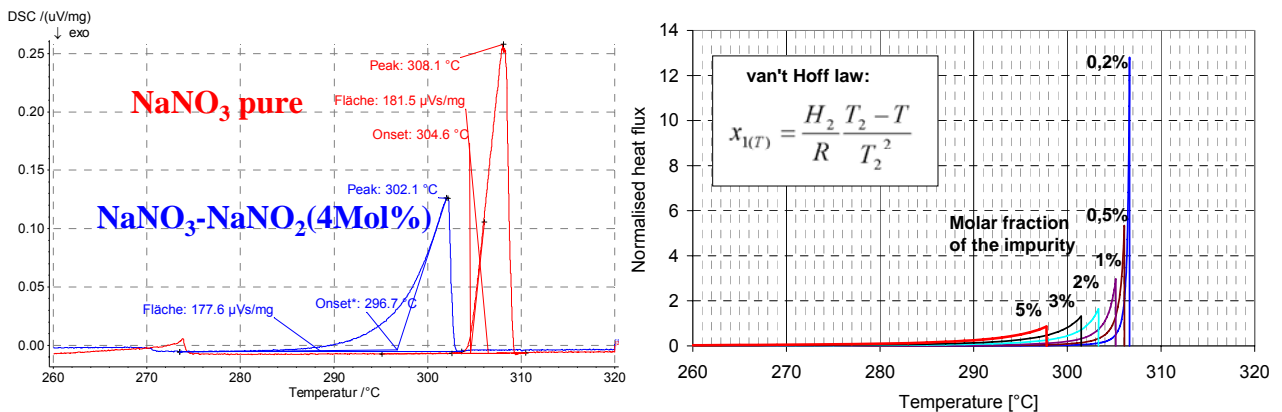


Figure 1: NaNO_3 with and without NaNO_2 impurity: DSC-measurement (left), calculated DSC-heat flux (right)

From the above discussion about NO_2^- in NaNO_3 it can be concluded that heating of the PCM far above the melting temperature may lead to some constraints, since the NO_2^- leads to a change in the NaNO_3 melting behaviour. Here, the kinetics of the equilibrium reaction may or may not allow full oxidation of the nitrite to nitrate on cooling.

At **high temperatures** (above about 700°C), further decomposition takes place with the evolution of the oxides of nitrogen in the gas phase. Here, KNO_3 has been found slightly more stable compared to NaNO_3 and the eutectic $\text{KNO}_3\text{-NaNO}_3$ [8,10,15]. Experimental difficulties with salt creeping have been reported. At temperatures large than 500°C creeping salt in contact with materials such as stainless steel or quartz leads also to the liberation of nitrogen oxides [8].

In the following the discussion of the three temperature regimes is summarised. Figure 2 shows the nitrite concentration in different alkali metal nitrates depending on the temperature. Although data below 350 °C are limited, own measurements and work by Kust show that the nitrite formation at this temperature is below 0.5 wt%. Hence, for the PCM application, if a maximum temperature of 350 °C is assumed, changes in the melting behaviour of NaNO₃ can be neglected.

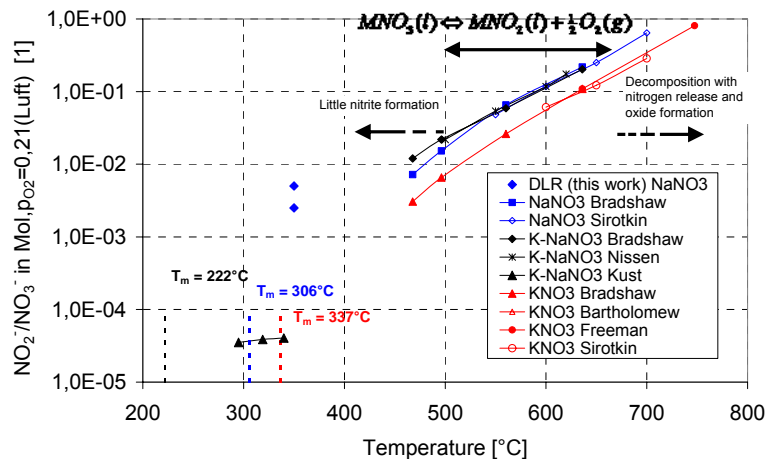


Figure 2: Literature and DLR measurement data of the nitrite concentration in alkali metal nitrates.

4. COMPATIBILITY OF MOLTEN SODIUM NITRATE AND GRAPHITE

NaNO₃ has a low thermal conductivity and this leads to a limited charge and discharge power of storage systems. Various methods have been proposed to enhance the heat transfer of the poorly conducting PCMs. They include the encapsulation of the PCM, the development of composite materials and the use of heat transfer enhancement structures in the PCM [1]. The concept using heat transfer enhancement structures was successfully demonstrated and showed high heat transfer rates. As structural material graphite foil is promising. This foil is advantageous in terms of a high conductivity, a low density and its economics. In the following experiments of the chemical compatibility of molten NaNO₃ and this foil are discussed.

Literature data about the stability of graphite in molten NaNO₃ is limited. Abald reports about the incompatibility of molten NaNO₃ with graphite at 310 °C without further reference [18]. Also, it was found that nitrate salts oxidize graphite seals at temperatures above about 350 °C [19]. Below 300 °C graphite seals show a good compatibility with molten KNO₃-NaNO₃ [12].

In the following we report about own compatibility experiments of NaNO₃ and graphite foil. In the experiments technical grade NaNO₃ with a purity of at least 98 % supplied by SQM (type SSI) was used. The major impurities are chlorides (0.48), sulphates (0.15) and nitrites (0.02) with maximum values in percent. For oven tests graphite foil supplied by SGL was used (type F05010Z). This foil had a mass of about 3 g, a density of about 1 g/cm³ and the dimensions 30x2x0.05 cm. For thermogravimetric (TG) measurements, ground expanded graphite was purchased from SGL Carbon (type GFG50). This powder has a d₅₀ value of about 50 µm.

TG measurements were conducted at atmospheric pressure in argon with a heating rate of 5 K/min with a commercial system (Netzsch STA 449). For gas analysis, this system is coupled to a quadrupole mass spectrometer via a SiO₂ capillary tube (Netzsch QMS 403C). Reference measurements of the single salt and the single graphite showed no significant mass loss. The TG-measurement in Figure 3 on the left hand side shows that there is a mass loss of a NaNO₃-graphite powder blend at around 350 °C. In addition, gas evolution from about 300 °C can be

detected by the mass spectrometer. We repeated this compatibility test with p.a. grade NaNO_3 with no significant difference compared to the technical salt.

Oven experiments were carried out at atmospheric pressure in air at constant temperature. The graphite foil was fully immersed in 100 g NaNO_3 melt and weight down with an alumina disc. The crucible material was borosilicate glass. Figure 3 on the right hand side shows the mass loss versus time related to the initial total mass of NaNO_3 and graphite. The mass loss at 350 °C due to the oxidation of the graphite in the melt is clearly visible. At 310 °C the rate is much smaller, but extrapolation of the experiment leads to a rate of about 6 wt% per year. In addition, a follow-up examination of the salt by DSC showed that there was a significant broadening of the melting peak and a reduction of the melting temperature of about 20 K. For the PCM-storage application, it can be concluded that such a rate would not be acceptable.

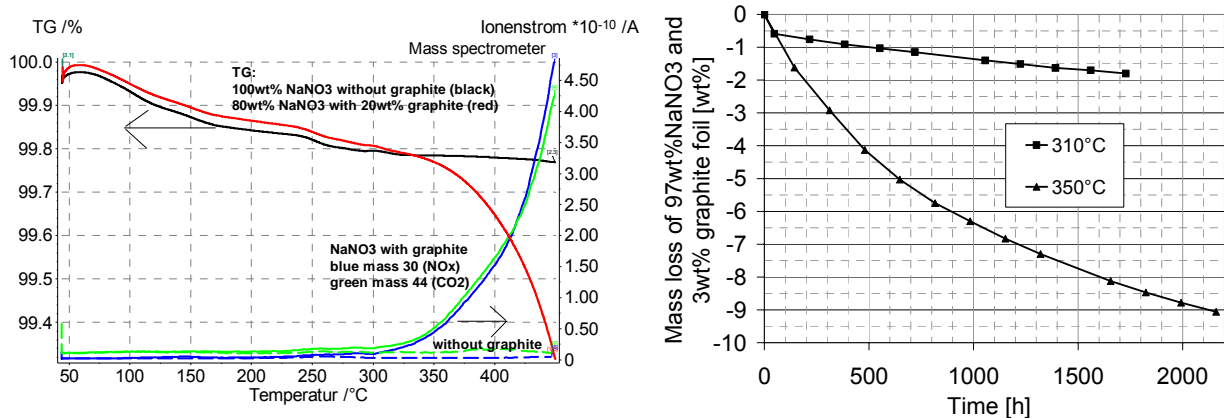


Figure 3: Stability of molten NaNO_3 and graphite; thermogravimetry with gas analysis (left) and oven test (right)

5. THERMOPHYSICAL PROPERTIES OF SODIUM NITRATE

The **density** of NaNO_3 at room temperature is well known with a value of 2.260 g/cm³ at 25 °C [20]. Literature data of the linear expansion coefficient in the solid state are also available. For polycrystalline NaNO_3 , the room temperature value is 40E-6 1/K [21]. The linear expansion coefficient increases steadily up to a maximum at the solid-solid conversion of NaNO_3 at around 275 °C. For higher temperatures, up to the melting temperature, the coefficient drops again [20, 22]. Using this literature expansion data, we calculated the density in the solid state from room temperature up to the melting temperature (Figure 4). Petitet reviewed data about the volume change on melting ΔV related to the volume in the solid state at the melting temperature at atmospheric pressure V_s and reported the following $\Delta V/V_s$ values in percent: 8.3, 9.6, 9.7, 10.0 and 10.7 [23]. In this work a value of 9.7 % from Schinke was assumed (Figure 4)[24]. This value is also the average of the five reported numbers. Figure 4 shows that the approach to calculate the liquid density at the melting temperature from the room temperature density, the linear thermal expansion coefficient and the volume change on melting is consistent with available literature data in the liquid range [25-29].

Heat capacity data of NaNO_3 are available from various authors and have been reviewed by Jirri (Figure 4)[6,21]. Original publications have been obtained and references are listed by Jirri. There is some discrepancy between older values mainly measured by drop calorimeters and newer values measured by DSC. Older values, in particular in the liquid range, are higher. Nguyen-Duy used a drop calorimeter and these exceptionally high values are not included here. Own measurements of the heat capacity were made with a heat flux type DSC (Netzsch DSC404) in Argon flow (100 ml/min) with a heating rate of 10 K/min. NaNO_3 was purchased from Merck

(purity 99,99 %) and used without further purification. The sample mass of about 20 mg was checked before and after the DSC measurement with a microbalance. Aluminium crucibles with a lid were used. Sapphire was utilized as heat capacity reference material with heat capacity data recommended by Netzsch. Figure 4 shows the average values from six newly prepared measurements. The maximum deviation from all measurements was +/- 4 % of these average values. For a temperature range from 80 to 190 °C and from 350 to 380 °C, the own measurement agrees to within +/-3 % with literature values from Rogers, Takahashi, Carling and Jriri [6]. The heat capacity in the liquid range is approximately constant, but measurements at high temperatures are difficult for two reasons. First, NaNO₃ in the liquid state strongly wets common container materials. As a result, the salt creeps out of the container [9,30]. Second, there is nitrite formation in the melt, so that measurements refer to the binary NaNO₂-NaNO₃ system.

The **thermal diffusivity** was measured by a variety of methods. They include the hot wire method using an insulating coating [31], optical techniques [32,33] and the stepwise heating method [34-36], as well as laser flash methods using two-layer [37] and three-layer arrangements [38]. In the liquid range at the melting temperature, the average of all this values is 0.163 mm/s. This value agrees with the calculated value using the relation $a = k/(\rho \cdot c_p)$. With the exception of measurements by Kobayasi [36], no work in the solid range could be identified (Figure 4). Own thermal diffusivity measurements of NaNO₃ in the liquid and solid state were carried out by the laser flash method using a three layer arrangement with a platinum crucible and a commercial apparatus (Netzsch LFA457). A single laser pulse beam illuminates the bottom area of a platinum crucible. The heat penetrates through three layers: the platinum crucible (thickness 0.30 mm), an either liquid or solid salt sample (0.66 mm, diameter 12 mm) and the platinum lid (0.31 mm). The bottom and top of this crucible were coated with a thin graphite layer in order to enhance the absorption and emission. The temperature rise versus time at the rear surface of the lid is measured by a liquid nitrogen cooled InSb photocell. The atmosphere was nitrogen (100 ml/min). A mathematical model describes the temperature rise versus time signal and was fitted to the experimental data using a non-linear regression algorithm. This three layer model includes the thicknesses of the three layers and thermophysical properties of the layers, as well as a correction of the heat losses and the laser pulse length. First, the compressed salt powder was melted in the crucible. Subsequently, the thermal diffusivities in the liquid and then in the solid state were measured isothermally. Three measurement series with a newly prepared crucible fill and three shots per temperature were carried out. The reproducibility in the liquid state was generally high. Virtually all single shots had an error smaller +/-5 % compared to the overall average. The salt layer thickness is the major cause of measurement uncertainty. For example an error of 0.01 mm in thickness leads to an error of 3 % in the diffusivity value. The reproducibility in the solid state was rather poor, so that the measurements can only give an indication of the diffusivity. Before and after the measurement series, the accuracy of the layer arrangement was verified by pure water measurements at room temperature compared to a literature value [21].

A comprehensive review and a recommendation of the **thermal conductivity** of molten NaNO₃ has been given by Nagasaka. Original publications and data have been obtained, but literature references are not listed here and are given by Nagasaka [36,39,40]. The recommended value is rather low, since many other high values are thought to include systematic errors due to radiation and convection [39]. Solid state values differ widely, so that no consistent data could be identified. One possible reason for this discrepancy may be differences in the crystal structure in solid NaNO₃ (e.g. single or polycrystalline).

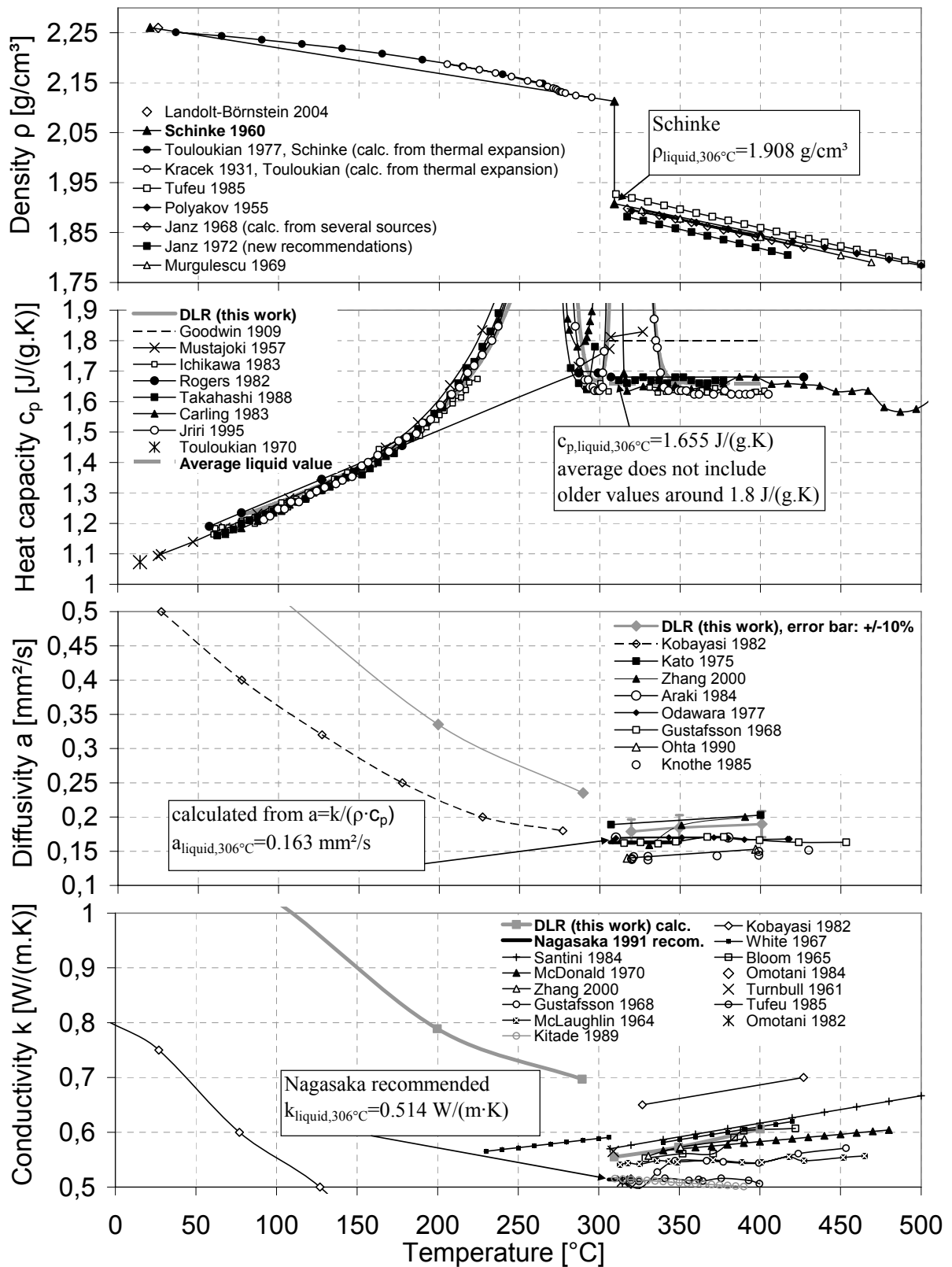


Figure 4: Thermophysical properties of solid and liquid NaNO₃; the melting temperature of NaNO₃ is 306 °C.

6. SUMMARY AND CONCLUSIONS

This paper focused on fundamental material aspects of sodium nitrate (NaNO_3) as a PCM for latent heat storage. The impact of **nitrite formation** in the NaNO_3 melt on the PCM utilisation has been examined. Literature values show that NaNO_3 melts form considerable amounts of nitrite in the temperature range from 450 to 700 °C. The examinations show that NaNO_2 in molten NaNO_3 results in a reduction of the NaNO_3 melting temperature. Hence, the maximum temperature of NaNO_3 utilised as a PCM is limited. Own long-term measurements show that NaNO_3 at 350 °C is thermally stable and nitrite formation can be neglected. Experiments on the **compatibility of molten NaNO_3 and graphite foil** have been also presented. Results show that the molten NaNO_3 slowly oxidizes graphite foil at 310 °C. This prohibits the long-term use of graphite foil in the NaNO_3 melt. **Thermophysical properties** of NaNO_3 in the liquid and solid range have been reviewed. Own measurements on the heat capacity and the thermal diffusivity have been presented. In the liquid range at 306 °C, consistent thermophysical data according to the relation $k = a \cdot \rho \cdot c_p$ have been identified. In the solid range, reliable density and heat capacity data are available, but there is a lack of consistent diffusivity and conductivity values. Measurements show that the diffusivity drops from room temperature to the melting temperature. Near the melting temperature, similar values in the solid and liquid range are observed.

REFERENCES

1. Tamme, R. et al. (2007) International Journal of Energy Research, 32, pp. 264-271.
2. Bauer, T. et al. (2008) Paper ID 163, Proc. Eurosun, 7-10th Oct., Lisbon.
3. Laue, W. et al. (1998) Nitrates and Nitrites, Ullmann's Encyclopedia of Industrial Chemistry, 6. Edition.
4. Pokorny, L. et al. (2006) Kirk-Othmer Encyclopedia of Chem. Techn., 22, Sodium nitrate and nitrite 5. Edition.
5. Lumsden, J. (1966) Thermodynamics of Molten Salt Mixtures, Chp. 6, Academic Press, pp. 109-132.
6. Jiriri, T. et al. (1995) Thermochemica Acta, 266, pp. 147-161.
7. Sabbah, R. et al. (1999) Thermochemica Acta 331, pp. 93-204.
8. Nissen, D.A. et al. (1983) Inorganic Chemistry, 22(5), pp. 716-721.
9. Kramer, C.M. et al. (1982) Thermochemica Acta, 55, pp. 11-17.
10. Freeman, E.S. (1957) Journal of the American Chemical Society, 79(4), pp. 838-842.
11. Bartholomew, R.F. (1966) The Journal of Physical Chemistry, 70(11), pp. 3442-3446.
12. Bradshaw, R. W. et al. (1987) Report, Sandia National Laboratories, SAND87-8005.
13. Kust, R.N. et al. (1970) Inorganic and Nuclear Chemistry Letters, 6, pp. 333-335.
14. Paniccia, F. et al. (1973) The Journal of Physical Chemistry, 77(14), pp. 1810-1813.
15. Sirotkin, G.D. (1959) Russian Journal of Inorganic Chemistry, 4(11), pp. 1180-1182.
16. Plambeck, J.A. (1976) Encyclopedia of electrochemistry of the elements, Vol. X, Marcel Dekker, pp. 189-232.
17. Bader, R.G. et al. (1993) Thermochemica Acta, 229, pp. 85-96.
18. Abald, E.R. (1968) Corrosion Guide, Elsevier.
19. Moreno, J., et al. (2003) Presentation, NREL Trough Thermal Storage Workshop, Golden, Feb. 20-21.
20. Gesi, K. (2004) 30 KNO₃ family, Landolt-Börnstein, Condensed Matter, New Series III/36B1, Springer.
21. Touloukian, Y.S. et al. (1979) Thermophysical Properties of Matter, Vol. 5, 10, 13, Plenum.
22. Kracek, F. C. (1931) Journal of the American Chemical Society, 53(7), pp. 2609-2624.
23. Petitot, J.P. et al. (1982) International Journal of Thermophysics, 3(2), pp. 137-155.
24. Schinke, H., et al. (1960) Zeitschrift für anorganische Chemie, 304, pp. 25-36 (in German).
25. Tufeu, R. et al. (1985) International Journal of Thermophysics, 6(4), pp. 315-330.
26. Polyakov, V.D. et al. (1955) Izvest. Siktora, Fiz.-Khim. Anal., 26, pp. 164-172 (in Russian).
27. Janz, G.J. et al. (1968), National Standard Reference Data Series, NSRDS 15.
28. Janz, G.J. et al. (1972) Journal of Physical and Chemical Reference Data, 1(3), pp. 581-746.
29. Murgulescu, I.G. et al. (1969) Electrochimica Acta, 14, pp. 519-526.
30. Rogers, D.J. et al. (1982) Journal of Chemical & Engineering Data, 27, pp. 424-428.
31. Zhang, X. et al. (2000) International Journal of Thermophysics, 21(1), pp. 71-84.
32. Gustafsson, S.E. (1968) Zeitschrift für Naturforschung, 23a, pp. 44-47.
33. Odawara, O. et al. (1977) Journal of Chemical and Engineering Data, 22(2), pp. 222.
34. Araki, N. (1984) International Journal of Thermophysics, 5(1), pp. 53-71.
35. Kato, Y. et al. (1975) Journal of Physics E: Scientific Instruments, 8, pp. 461-464.
36. Kobayasi, K. et al. (1982) Proc. 7. International Heat Transfer Conference, 6, pp. 467-472.
37. Knothe, W. (1985) Entwicklung einer Apparatur zur Messung der Wärmeleitfähigkeit von Schmelzen, doctoral thesis, RWTH-Aachen (in German).
38. Ohta, H. et al. (1990) Review of Scientific Instruments, 61(10), pp. 2645-2649.
39. Nagasaka, Y. et al. (1991) International Journal of Thermophysics, 12(5), pp. 769-781.
40. Zhang, X. et al. (2000) International Journal of Thermophysics, 21(1), pp. 71-84.